COMPUTATIONAL CONTINUUM MECHANICS

ВЫЧИСЛИТЕЛЬНАЯ МЕХАНИКА СЛОШНЫХ СРЕД

Computational Continuum Mechanics. 2021. Vol. 14. No. 4. pp. 398-412 DOI: 10.7242/1999-6691/2021.14.4.33

TWO-LEVEL ELASTOVISCOPLASTIC MODEL: ANALYSIS OF THE INFLUENCE OF CRYSTALLITE ORIENTATION DISTRIBUTION IN THE REFERENCE CONFIGURATION AND THE COMPLEXITY OF LOADING ON THE BEHAVIOR OF POLYCRYSTALLINE MATERIALS

P.V. Trusov and A.S. Sokolov

Perm National Research Polytechnic University, Perm, Russian Federation

Components and structural elements used in modern technology are often exposed to significant loads in a wide range of temperature and deformation rates, and are subjected to complex loading. As a result, all these factors put forward increased requirements for the properties of materials when designing structures of different sizes - from miniature to large-scale. A significant part of the structures used in various industries is made of polycrystalline metals and alloys. The physical and mechanical properties of polycrystalline aggregates in finished products depend on their phase and component composition, meso- and microstructure, including the orientation of crystallites (grains, subgrains), symmetry properties of the latter, and on the initial (residual) stresses that occur during their manufacturing. Since experimenting with full-scale structures requires considerable material and time expenditures, mathematical modeling approaches are applied for designing structures and their manufacturing processes. Mathematical modeling provides an opportunity to describe processes in any materials with varying degrees of accuracy. Constitutive relations (or constitutive models) are the most important element of the mathematical models developed for solving these problems. Currently, the most promising among these models are multilevel models based on the introduction of internal variables and crystal plasticity. When analyzing the elastic-plastic deformation of various products, the isotropic constitutive relations are often used to simplify the analysis of the elastic component of deformations. This work is devoted to the study of errors arising when the anisotropic elastic properties of crystallites are replaced by the corresponding isotropic properties of the materials with BCC, FCC and HCP lattices for different laws of orientation distribution of crystallites in a polycrystalline aggregate in a reference configuration. Using a two-level model based on the physical theory of elastoviscoplasticity, a series of numerical experiments on simple shear loading, sequences of two simple loads, and cyclic deformation was performed to analyze the evolution of the stress-strain state and to estimate the residual stresses in crystallites.

Key words: two-level physical elastic-viscoplastic model, equivalent isotropic material, residual mesoscopic stresses, crystallographic texture

1. Introduction

Despite the increasing use of composite materials in various branches of industry, metals and alloys remain among the main structural materials. The development of technological regimes for processing alloys in recent decades is based on mathematical modeling of inelastic deformation processes in a wide range of thermomechanical effects. At the same time, most models focused on solving practical engineering problems are based on the macrophenomenological theories of plasticity, elastoviscoplasticity, and creep [1–6]. However, these theories were elaborated using the results of macroexperiments (mainly, uniaxial loading tests), and therefore they do not explicitly describe the physical mechanisms responsible for structural changes in materials at various structural-scale levels. At present, there is a large amount of experimental data and theoretical studies which provide evidence that the processes of inelastic deformation and the properties of polyscrystalline materials at the macrolevel are determined primarily by the state of the evolving meso- and microstructure of the material. Therefore, multilevel models with substantial universality based on the introduction of internal variables and physical theories of inelasticity (elastic plasticity, elastoviscoplasticity) have gained wide recognition [7-11].

In the last 15-20 years, in order to improve the physical and mechanical properties of products made of metal and alloys, the use of processing by means of severe plastic deformation (SPD) has become relevant in industry and mechanical metallurgy engineering, which makes it possible to obtain materials with unique properties: submicrocrystalline, nanocrystalline, textured materials,

Email addresses for correspondence: tpv@matmod.pstu.ac.ru

materials capable of undergoing superplastic deformation, etc. Numerous studies have shown that the products deformed through SPD have improved performance properties, the acquisition of which is a consequence of significant changes in the meso- and microstructure of the material, such as grain shaping, crushing and fragmentation, rotation of the crystalographic lattices of subgrains and fragments, and dislocation substructure evolution.

To improve existing technologies and develop new SPD ones, in order to obtain materials and products with improved performance characteristics, it is necessary to construct constitutive models for describing the evolution of the structure during deformation, taking into account the effect of the changes in the structure on the process parameters and the effective properties of the material at the macroscale level. Multilevel models with internal parameters mentioned above become popular because they fully meet these requirements and can be used to create advanced functional materials [11].

Multilevel models are subdivided by the number of considered levels, the type of constitutive relations at the lower structural-scale level, and by the hypotheses about the relationship between the related parameters of different levels. There are three main groups of multilevel models: direct, self-consistent, and statistical [11]. To date, the most commonly used models are statistical two-level (including meso- and macrolevels) elastic viscoplastic models originating in the works of Taylor [12] and Lin [13]. One of these statistical models will be used in this study.

It should be noted that the study of SPD technologies requires the formulation and solution of boundary value problems, and the analysis of the geometric nonlinearity of boundary conditions, kinematic and constitutive relations (CR). One of the basic equations of the model is the elastic law, formulated in most cases in the rate relaxation form. In this case, the assumption about the isotropy of elastic properties is often accepted both at the macro- and mesolevels. A similar hypothesis can still be accepted at the macrolevel for polycrystalline metals using a uniform law of distribution of grain lattice orientations, but it is hardly acceptable at the mesolevel (the level of individual crystallites - grains, subgrains). In this regard, the question arises of estimating the errors caused by the assumption of the anisotropy of elastic properties both at the level of a representative macrovolume and at the level of crystallites.

It should be mentioned that, when describing plastic deformation in physical theories of elastoviscoplasticity, the anisotropy of crystallites is naturally considered. Previously, the authors analyzed the correspondence between stress-strain states (SSS) (including residual stresses in a representative macrovolume exposed to complete unloading) that comply with the anisotropic and equivalent isotropic elastic characteristics obtained under simple loading conditions. It was assumed that polycrystalline samples have three different types of lattices with an initial uniform distribution of lattice orientations [14]. This paper presents the results of studies for arbitrary complex loading of polycrystalline samples with different laws of distribution of crystallite orientations in the reference configuration.

2. Mathematical formulation

In this study, the problem of SSS determination is solved in terms of a two-level elastoviscoplastic model [11]. The representative macrovolume of a polycrystal acts as an element of the macrolevel, that is the minimum volume of a crystallite (grains, subgrains). An increase in the number of crystallites in this case will not cause any significant deviations in the analyzed parameters of this level, for example, the relations between stress intensity and accumulated plastic strain intensity. A crystallite (grain, subgrain) is considered as an element of the mesolevel. The main mechanism of deformation is the motion of boundary dislocations along slip systems known for each lattice type. Hardening on the slip systems and rotations of crystallite lattices under loading are also taken into account.

One of the key questions related to the development of constitutive models able to describe the processes of deformation with high velocity gradients (analyzing geometric nonlinearity) is the decomposition of motion into quasi rigid and strain-induced motions, which should allow taking into account the symmetric properties of crystallites [15]. For this purpose, a moving non-deformable

orthogonal Cartesian coordinate system (MCS) $Ox^1x^2x^3$ with a basis $\mathbf{k}^i$ that is rigidly connected with a crystallographic direction and a crystallographic plane containing this direction is introduced for each mesolevel element (crystallite) [16, 17]. In the framework of the coordinate system rigidly connected with the crystallite lattice, the elastic tensor components $\mathbf{п}$ are assumed to be unchanged. An affine change in the configuration of each crystallite is determined by the mesoscale deformation gradient $\mathbf{f}$ [18, 15]. The additional unloaded configuration found from the reference configuration by applying transformation producing no changes in the lattice orientation (reference configuration – plastic component $\mathbf{f}^p$ of the deformation gradient, and actual configuration - transformation $\mathbf{f}^{e-1}$) is used to study both elastic and inelastic deformations. Along with the classical multiplicative decomposition of the deformation gradient $\mathbf{f}=\mathbf{f}^e\cdot\mathbf{f}^p$ [19, 20], the expansion proposed in [16, 17], is used as the main one: $\mathbf{f}=\overline{\mathbf{f}}^e\cdot\mathbf{r}\cdot\mathbf{f}^p$. Here, $\mathbf{f}^e$ is the elastic component of the deformation gradient, $\mathbf{r}=\mathbf{k}_i\mathbf{k}_0^i$ is the proper orthogonal tensor which converts the reference basis $\mathbf{k}_0^i$ of the moving coordinate system into the current basis, $\overline{\mathbf{f}}^e$ is the deformation gradient which transforms the plastically deformed configuration (subjected to rotation) into the actual configuration at the mesolevel, i.e., $\overline{\mathbf{f}}^e$ indicates the crystal lattice distortion. Based on this decomposition, the quasi-rigid crystal motion is described by the rotation tensor $\mathbf{r}$, which simultaneously defines the rotation of the rigid MCS.

The mathematical formulation of macro- and mesolevel submodels is given below (macroscale parameters are denoted by capital letters, and similar mesolevel parameters - by similar lowercase letters). The systems of equations take the form

- for macrolevel

$$\begin{cases}\mathbf{K}^{\mathrm{cor}}\equiv\dot{\mathbf{K}}-\boldsymbol{\Omega}\cdot\mathbf{K}+\mathbf{K}\cdot\boldsymbol{\Omega}=\boldsymbol{\Pi}:\left(\mathbf{L}-\boldsymbol{\Omega}-\mathbf{Z}^{\mathrm{in}}\right),\\ \boldsymbol{\Pi}=\left\langle\mathbf{п}\right\rangle,\\ \boldsymbol{\Omega}=\left\langle\boldsymbol{\omega}\right\rangle,\\ \mathbf{Z}^{\mathrm{in}}=\left\langle\mathbf{z}^{\mathrm{in}}\right\rangle+\boldsymbol{\Pi}^{-1}:\left\langle\mathbf{п}':\mathbf{z}^{\mathrm{in}'}\right\rangle+\boldsymbol{\Pi}^{-1}:\left(\left\langle\boldsymbol{\kappa}'\cdot\boldsymbol{\omega}'\right\rangle-\left\langle\boldsymbol{\omega}'\cdot\boldsymbol{\kappa}'\right\rangle\right);\end{cases}\tag{1}$$

– for mesolevel

$$\begin{cases}\boldsymbol{\kappa}^{\mathrm{cor}}\equiv\dot{\boldsymbol{\kappa}}+\boldsymbol{\kappa}\cdot\boldsymbol{\omega}-\boldsymbol{\omega}\cdot\boldsymbol{\kappa}=\mathbf{п}:\left(\mathbf{l}-\mathbf{z}^{\mathrm{in}}-\boldsymbol{\omega}\right),\\ \dot{\mathbf{r}}\cdot\mathbf{r}^{\mathrm{T}}=\boldsymbol{\omega},\\ \mathbf{z}^{\mathrm{in}}=\sum\limits_{k=1}^{K}\dot{\gamma}^{(k)}\mathbf{b}^{(k)}\mathbf{n}^{(k)},\\ \dot{\gamma}^{(k)}=\dot{\gamma}_0\left(\dfrac{\tau^{(k)}}{\tau_{\mathrm{c}}^{(k)}}\right)^m\mathrm{H}\left(\tau^{(k)}-\tau_{\mathrm{c}}^{(k)}\right),\\ \tau^{(k)}=\mathbf{b}^{(k)}\mathbf{n}^{(k)}:\boldsymbol{\kappa},\\ \dot{\tau}_{\mathrm{c}}^{(k)}=\sum\limits_{l=1}^{K}h^{(kl)}\,\dot{\gamma}^{(l)},\\ h^{(kl)}=\left[q_{\mathrm{lat}}+\left(1-q_{\mathrm{lat}}\right)\delta^{(kl)}\right]h^{(l)},\\ \begin{cases}\text{ОЦК, ГПУ:}\quad h^{(l)}=h_0^{(l)}\left(\dfrac{h_0^{(l)}\gamma^{(l)}}{\tau_{\mathrm{sc}0}^{(l)}n}+1\right)^{n-1},\\ \text{ГЦК:}\quad h^{(l)}=\mathrm{h}_0\left|1-\tau_{\mathrm{c}}^{(l)}/\tau_{\mathrm{sat}}\right|^{\mathrm{a}},\end{cases}\\ \mathbf{l}^e=\mathbf{l}-\mathbf{z}^{\mathrm{in}}.\end{cases}\tag{2}$$

Here, $\mathbf{K}$ ($\boldsymbol{\kappa}$) is the weighted Kirchhoff stress tensor at the macrolevel (mesolevel); $\mathbf{K}^{\mathrm{cor}} = \dot{\mathbf{K}} - \boldsymbol{\Omega}\cdot\mathbf{K} + \mathbf{K}\cdot\boldsymbol{\Omega}$ ($\boldsymbol{\kappa}^{\mathrm{cor}} = \dot{\boldsymbol{\kappa}} + \boldsymbol{\kappa}\cdot\boldsymbol{\omega} - \boldsymbol{\omega}\cdot\boldsymbol{\kappa}$) is the corotational rate of change of the weighted Kirchhoff stress tensor at the macrolevel (mesolevel), which is independent of choice of a reference frame; $\boldsymbol{\Omega}$ ($\boldsymbol{\omega}$) is the moving coordinate system spin tensor at the macrolevel (mesolevel); $\boldsymbol{\Pi}$ ($\boldsymbol{\pi}$) is the elastic tensor; $\mathbf{Z}^{\mathrm{in}}$ ($\mathbf{z}^{\mathrm{in}}$) is the inelastic component of the indifferent strain rate measure at the macrolevel (mesolevel) $\mathbf{Z} = \hat{\nabla}\mathrm{V}^{\mathrm{T}} - \boldsymbol{\Omega}$ ($\mathbf{z} = \hat{\nabla}\mathbf{v}^{\mathrm{T}} - \boldsymbol{\omega}$); $\mathbf{l} = \hat{\nabla}\mathbf{v}^{\mathrm{T}}$ is the transposed velocity gradient (by the Voigt's hypothesis $\mathbf{l} = \mathbf{L} = \hat{\nabla}\mathbf{V}^{\mathrm{T}}$, $\mathbf{L}$ — transposed velocity gradient at the macrolevel); $\dot{\gamma}^{(k)}$ is the shear rate on the k-th slip system; $\dot{\gamma}_0$ is the shear rate on the slip system when the tangential stress approaches the critical shear stress; $\tau^{(k)}$ and $\tau_{\mathrm{c}}^{(k)}$ are the resolved and critical stresses on the k-th slip system; $\tau_{\mathrm{sc0}}^{(l)}$ is the initial critical stress on the l-the slip system; τ_{sat} is the saturation stress; m is the strain rate sensitivity exponent of the material; $\mathrm{H}(\cdot)$ is the Heaviside function; $\mathbf{b}^{(k)}$, $\mathbf{n}^{(k)}$ are the unit vectors of the slip direction and the normal to the k-th slip plane in the actual configuration; $\mathbf{r}$ is the tensor of rotation of the MCS at the mesolevel; $\langle\cdot\rangle$ denotes the macro-volume averaging operator, $\mathbf{a}'$ shows the deviations of the tensor characteristic $\mathbf{a}$ for the crystallite from the value averaged by the representative macrovolume.

Let us consider an algorithm that makes it possible to implement the formulated two-level model for describing the deformation of the macrolevel representative volume of an elastic-plastic body (Fig.1). Loading is performed kinematically, $\mathbf{F}(t)$ is a continuous and continuously differentiable function. Due to the significant nonlinearity of the problem of studying deformation processes, a step-by-step time procedure is used for the solution, according to which the entire loading time interval is represented by a set of small-time steps. The main purpose of the calculations performed is to find, according to the prescribed law of deformation $\mathbf{F}(t)$ at each time step, the components of the stress tensors at the macro- $\mathbf{K}(t)$ and meso- $\boldsymbol{\kappa}(t)$ levels, as well as to determine the residual stresses in the crystallites.

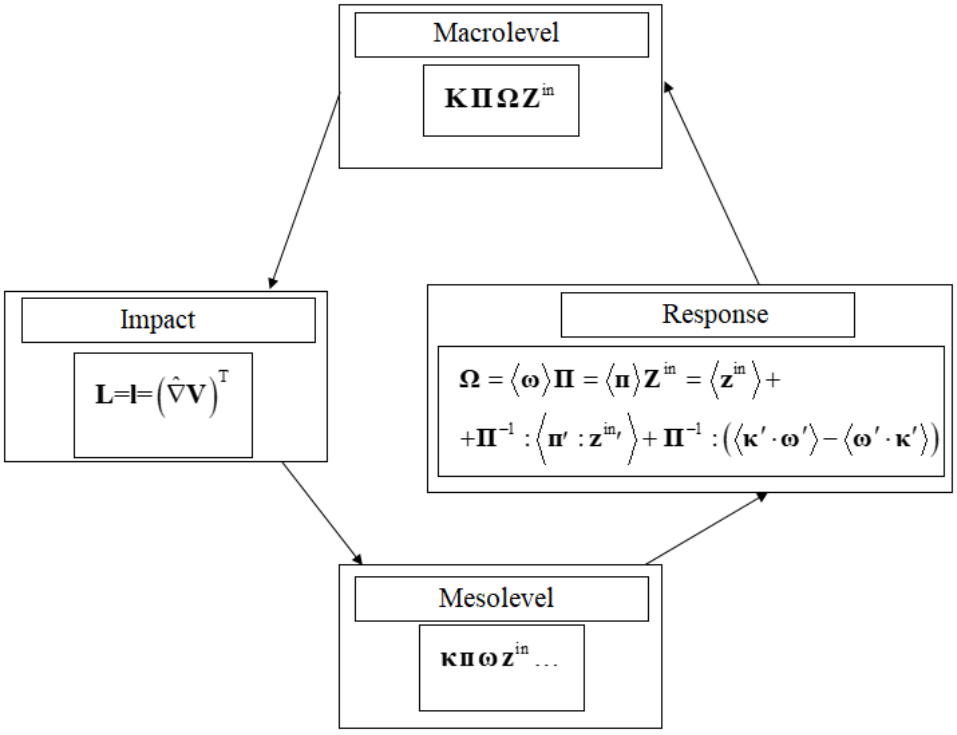

Fig.1. Scheme of the algorithm for a two-level elastic-viscoplastic model of the deformation process: arrows show the direction of transfer of parameters between the calculation procedures of different levels.

In the reference configuration, parameters of the following two groups are specified:

- model parameters (the number of crystallites in a representative macrovolume, the law of distribution of crystallite orientation, the law of change of the transposed place gradient);
- material parameters (the number of slip systems in a crystallite, initial critical stresses, hardening law, Burgers vectors and normal to the slip plane, elastic tensor components in a reference configuration that coincides with a crystallographic coordinate system (in the MCS basis) or equivalent isotropic elastic moduli).

It is assumed that the material in the reference configuration has a natural state, and the crystallite lattices are oriented in accordance with the prescribed distribution law:

$$\boldsymbol{\kappa}\big|_{t=0} = \mathbf{0}, \quad \boldsymbol{\tau}_{\mathrm{c}}^{(k)}\Big|_{t=0} = \boldsymbol{\tau}_{\mathrm{c}0}^{(k)}, \qquad \gamma^{(k)}\Big|_{t=0} = 0 \quad \left(k = 1,...,K\right), \qquad \mathbf{r}\big|_{t=0} = \mathbf{r}_0 .$$

At each time step (at its beginning), all calculation parameters (actual and critical stresses, accumulated shifts, lattice orientations, etc.) are assumed to be known from the previous step. Let us note the solution at the first step, which should be implemented with a relatively small time step. This is attributed to the fact that in the initial configuration the material is in its natural state; the stress tensors for each crystallite are thus equal to the zero tensor. Therefore, no stress relaxation can occur in this case under inelastic deformation. In this case, too large time steps can lead to very high stresses, and as a result, can even cause the oscillation of the solution. Subsequent loading steps are implemented in the elastoplastic region, where stress relaxation occurs due to inelastic deformations.

The step-by-step algorithm that describes the loading of a representative macrovolume includes sequential fulfillment of the following points:

Step1: mesolevel (for each crystallite):

a Calculation in rates:
  i. components of the velocity gradient tensor $\mathbf{l}$ are defined in the MCS basis;
  ii. plastic component of the strain rate measure is determined;
    1. tangential stresses on each slip system are calculated;
    2. shear rates are determined for each slip system;
  iii. changes in the critical tangential stresses are evaluated;
  iv. spin tensor and plastic component of the strain rate tensor are calculated;
  v. stress tensor derivative is determined using Hooke's law in the rate relaxation form.

b Integration (determination of unknown variables corresponding to the completed current step):
  i. calculation of accumulated shear on each slip system.
  ii. calculation of critical stresses;
  iii. determination of MCS rotation step increments;
  iv. calculation of a stress tensor at the mesolevel.

Step II: macrolevel

a spin and elastic tensor components and strain measure plastic component are calculated in the laboratory coordinate system (LCS) basis for each crystallite and then averaged; macrolevel spin tensors and elastic tensors are determined;

b stress tensor derivative at the macrolevel is calculated using Hooke's law in the rate relaxation form.

c stress tensor at the macrolevel is established.

The efficiency of the developed algorithm and program for its implementation has been verified by the results obtained during a simple shear test on a titanium sample. A brief review of recent full-scale studies on the deformation of titanium single crystals was carried out to search for the data necessary in computational experiments. In a number of publications for various loading of titanium crystallites data are given that could be acceptable for identifying multilevel models. In [21], the quasi-static loading of a sample made of alpha- and beta-titanium (the β phase interlayer is in the middle of the sample) was considered. Dynamic compression of titanium single crystals was discussed in [22]. In [21, 23, 24], the compression of a titanium single crystal in a structure consisting

of titanium base samples, a substrate, and a loading setup was studied. Individual characteristics of the considered samples are not given.

The accuracy of the numerical results obtained using the proposed algorithm was tested when comparing with the results of the simple shear test described in [25] (Fig.2). The independent elastic tensor components (constant in the MCS basis), in terms of which the remaining components are expressed, are as follows

$$\text{п}_{11}=162,4\ \text{GPa},\quad \text{п}_{33}=180,7\,\text{GPa},\quad \text{п}_{12}=92\ \text{GPa},\quad \text{п}_{13}=69\ \text{GPa},\quad \text{п}_{55}=46,7\ \text{GPa},$$

where the symmetric 4th rank tensor is written in matrix form (followed by the Voigt notation). The initial critical stresses used in our calculations are 150 MPa for basis slip type, 30 MPa for prismatic slip type, and 120 MPa for pyramidal $\langle c+a\rangle$ slip type [26]. Other parameters are as follows: $\dot{\gamma}_0=0,0001\text{s}^{-1}$; $\dot{\gamma}_{0tw}=0,001\text{s}^{-1}$ is the twin shear rate at the tangential stress that equals the critical stress; $m=50$ [26]. Kinematic loading parameters are defined by the deformation gradient: $\mathbf{f}(t)=\mathbf{F}(t)=\mathbf{E}-\gamma\,\mathbf{p}_2\mathbf{p}_3=\mathbf{E}-\dot{\varepsilon}\,t\,\mathbf{p}_2\mathbf{p}_3$, where $\dot{\varepsilon}=0,0017\ \text{s}^{-1}$, $\mathbf{p}_i$ is the laboratory coordinate system basis [25]. The step-by-step implementation procedure was realized at the time step $\Delta t=0,0001\,\text{s}$ corresponding to the strain increment $\Delta\varepsilon=0,0001$.

The step size in this example, and those considered below, was determined from preliminary numerical experiments and chosen according to the condition of an insignificant difference in the results of calculations at two adjacent time steps. It should be noted that, from now on, due to the small integration steps, the graphs plotted by points are represented by continuous lines. The sample used in this experiment was a single crystal with the MCS orientation that coincides with the LCS orientation; the results of the calculations are given in Fig.2.

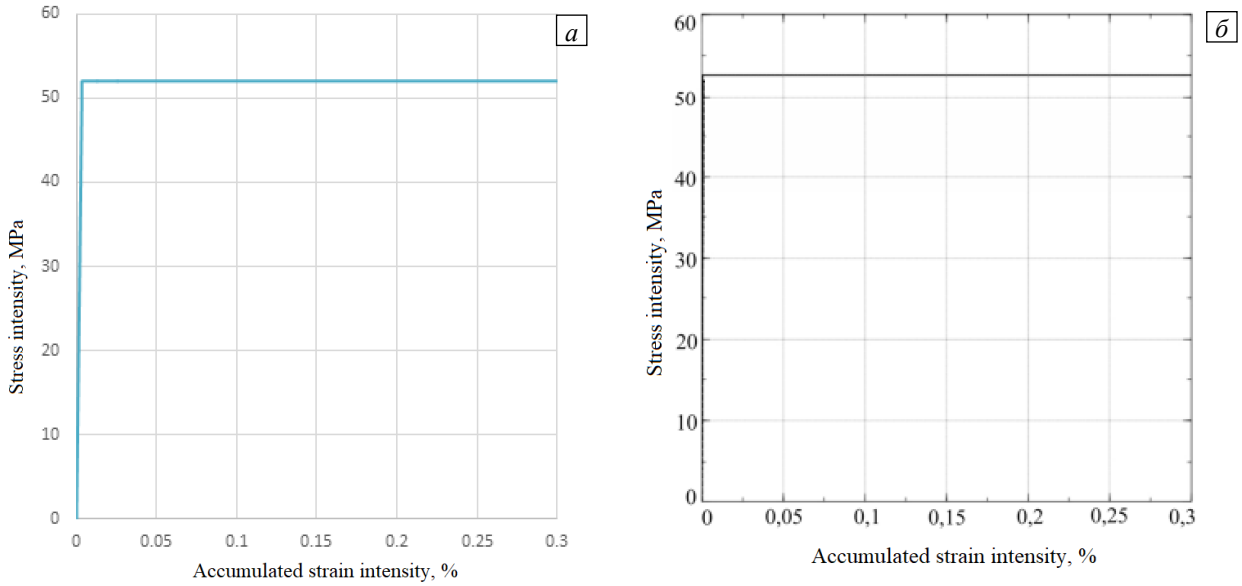

Fig.2. The dependence of stress intensity on accumulated strain intensity for the crystallite with anisotropic properties: calculations performed using the proposed model (1), (2) (a), results from [25] (b).

3. Input data for computational experiments

The elastic properties of materials are determined by the elastic fourth rank tensor. A transition from tensor to the matrix form is carried out using the Voigt notation; a correspondence between the first and second pairs of indices of the fourth rank tensor components and the elastic matrix components (dimension 9 × 9) is illustrated by the relations:

$$11 \to 1; \quad 22 \to 2; \quad 33 \to 3;$$
$$23 \to 4; \quad 31 \to 5; \quad 12 \to 6;$$
$$32 \to 7; \quad 13 \to 8; \quad 21 \to 9.$$

The independent nonzero components of the elastic tensor (according to the Voigt's notion) in the MCS basis for single crystals (mesolevel elements) of alpha iron (bcc lattice) [27], copper (fcc lattice) [16, 28], titanium (hcp lattice) [26] are equal:

$$\text{BCC:} \quad \text{п}_{11} = 200 \text{ hPa}, \quad \text{п}_{12} = 137 \text{ hPa}, \quad \text{п}_{66} = 116 \text{ hPa};$$
$$\text{BCC:} \quad \text{п}_{11} = 168,4 \text{ hPa}, \quad \text{п}_{12} = 121,4 \text{ hPa}, \quad \text{п}_{44} = 75,4 \text{ hPa};$$
$$\text{HCP:} \quad \text{п}_{11} = 162,4 \text{ hPa}, \quad \text{п}_{33} = 180,7 \text{ ГПа hPa}, \quad \text{п}_{12} = 92 \text{ hPa}, \quad \text{п}_{13} = 69 \text{ hPa}, \quad \text{п}_{55} = 46,7 \text{ hPa}.$$

Using the components of the tensor describing the elastic properties of crystallites and under the assumption of a uniform distribution of crystallite orientations, the elastic moduli of isotropic continuums are calculated by the Voigt-Reuss-Hill averaging [28–33]. The obtained results are given in Table 1. It should be recalled that the description of inelastic deformations at the mesolevel is based on the consideration of the crystal structure of the elements of this level, and in this connection, the terms "crystallite", "mesolevel element orientation", even under the assumption of isotropic elastic properties, make sense.

Table 1. Model parameters and calculated values of the elastic moduli for isotropic materials.

Material, lattice, parameters	Averaging technique	K, hPa	μ, hPa	λ, hPa
alpha iron, bcc $\dot{\gamma}_0 = 10^{-5}\,\text{s}^{-1}$; $m = 83,3$; $q = 1,3$; $n = 0,58$; $\tau_{c0}^{(k)}\{110\} = 24$ MPa, $\tau_{c0}^{(k)}\{112\} = 112,8$ MPa, $\tau_{c0}^{(k)}\{123\} = 59,2$ MPa.	Voigt	308,07	78,76	255,56
	Reuss	308,07	41,88	280,15
	Hill	308,07	60,32	267,85
copper, fcc $\dot{\gamma}_0 = 10^{-9}\,\text{s}^{-1}$; $m = 89,3$; $q = 1$ (complanar cc), $q = 1,4$ (noncomplanar cc); $a = 2,25$, $\tau_{sat} = 148$ MPa, $\tau_{c0}^{(k)}\{112\} = 15$ MPa.	Voigt	137,07	54,64	100,64
	Reuss	137,07	33,33	114.,85
	Hill	137,07	43,98	107,74
titanium, hcp $\dot{\gamma}_0 = 10^{-4}\,\text{s}^{-1}$; $m = 50$; $q = 1,4$; $n = 0,53$; $\tau_{c0}^{(k)}\{0001\} = 150$ MPa, $\tau_{c0}^{(k)}\{10\bar{1}0\} = 30$ MPa, $\tau_{c0}^{(k)}\{10\bar{1}1\} = 120$ MPa.	Voig	107,06	44,00	78,02
	Reuss	123,54	38,23	98,31
	Hill	115,3	41,11	88,16

The numerically found integration step does not exceed the calculated $\Delta t = 0,0001$ s, which corresponds to the strain intensity incremental step $\Delta\varepsilon = 0,0001$.

The meso- and microstructural properties of the material evolves significantly in the process of deformation due to the impacts caused by stresses or by kinematic forces at the macrolevel. Thus, an opportunity to control of the meso- and microstructure evolution makes it possible to change the macrolevel properties of materials that provide specific performance characteristics of finished products [34, 35].

In modeling a simple shear, the transposed place gradient is given as

$$\mathbf{F}=\mathbf{l}_1\mathbf{l}_1+\mathbf{l}_2\mathbf{l}_2+\mathbf{l}_3\mathbf{l}_3+\lambda t\mathbf{l}_1\mathbf{l}_2, \tag{3}$$

where λ is the strain rate parameter, t is the time, $\mathbf{l}_i$, $(i\in\overline{1,3})$ are the basis vectors of the fixed laboratory coordinate system, which indicate the characteristic loading axes.

When the material under study is subjected to complex loading (combined simple shear/tension loadings), the transposed place gradient is described by the relation:

$$\mathbf{F}=\begin{cases}\mathbf{I}+\dot\gamma_{12}t\,\mathbf{l}_1\mathbf{l}_2, & t\in[0,1000]\,s,\\ \mathbf{I}+\langle t-1000\rangle\left(e^{0,5\lambda t}\left(\mathbf{l}_1\mathbf{l}_1+\mathbf{l}_2\mathbf{l}_2\right)+e^{-\lambda t}\mathbf{l}_3\mathbf{l}_3\right), & t\in(1000,\,2000]\,\text{s},\end{cases} \tag{4}$$

where $\langle x\rangle = x\,\mathrm{H}(x)$ is the Macaulay brackets, and $\mathrm{H}(\cdot)$ is the Heaviside function, $\lambda=0,001\ \text{s}^{-1}$, $\dot\gamma_{12}=0,005\,\text{s}^{-1}$.

In modeling cyclic loading, deformations is specified by the following transposed deformation gradient:

$$\mathbf{F}=\mathbf{l}_1\mathbf{l}_1+\mathbf{l}_2\mathbf{l}_2+\mathbf{l}_3\mathbf{l}_3+3\dot\varepsilon t\left(7\cos\left(\frac{7t}{T}\right)-\sin\left(\frac{7t}{T}\right)\right)\mathbf{l}_1\mathbf{l}_2+5\dot\varepsilon t\left(\cos\left(\frac{7t}{T}\right)+4\sin\left(\frac{7t}{T}\right)\right)\mathbf{l}_1\mathbf{l}_3, \tag{5}$$

where $\dot\varepsilon=10^{-4}\ \text{s}^{-1}$ is the constant parameter, and $T=1000\,\text{s}$ is the end time of deformation. As options for specifying the crystallite orientation distribution in the reference configuration, we use either a uniform law or the orientation distribution obtained after rolling (the data for polycrystals with HCP structure are taken from [36] (Fig. 3) and for polycrystals with BCC and FCC structures from [37]).

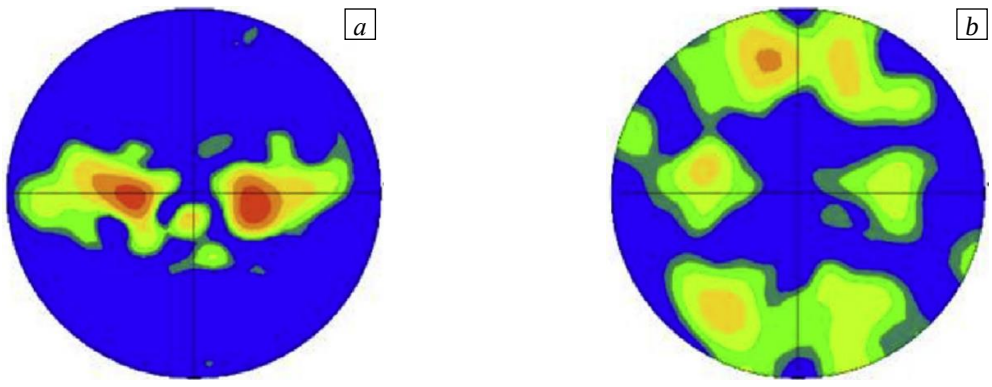

Fig.3. Pole figures showing the texture of the polycrystal titanium sample after rolling [36] for the orientation distribution of crystallographic planes $\{0001\}$ *(a)* and $\{10\bar{1}0\}$ *(b).*

4. Residual stresses

Residual stresses are stresses that exist in the bodies under study in the absence of external loads [38]. They arise in almost any metals after application of such technological processing techniques

as casting, forging, thermal and mechanical treatment [39]. Moreover, the residual stress intensity factor can approach the yield strength. In many cases, the failure of the structures made of high-strength metals is caused by a combination of different factors, namely, residual stresses occurred in materials during the manufacture process and stresses induced in turbine blades, compressors, crankshafts, plungers, etc. [40]. Special heat treatment, although having a chance to reduce residual stresses, is not always possible, e.g., in the case of large size products. It should be noted that the performance degradation of parts will not in any case be associated with residual stresses because some technological processes (blasting with shot, rolling with rollers, etc.) provide for the creation of residual stresses [38, 40]. For these reasons, the development of technologies that allow producing residual stresses to improve the performance properties of metal products is an important task. Theoretically, residual stresses can be "induced" so that one can obtain the best characteristics of metal products in prescribed directions (for example, the initial flow stresses are greater in the direction of tension than in the direction of compression, or vice versa). That makes it possible to process metal ingots in such a way that the level and/or distribution of residual stresses in finished products will become optimal (for specific operating conditions).

The main property of residual stresses is their self-balance. According to the structural-scale levels at which this property manifests itself, they can be classified into type I, II and III [41, 42]. Residual stresses of type 1 (macroscopic) arise during mechanical and thermal treatment, in particular, due to phase transformations of metals [41, 39]. They are balanced in the entire volume of the detail, but not equal to zero in its individual parts. Residual stresses are induced by the incompatibility of elastic deformations caused by the inhomogeneity of the force and temperature fields occurred in the details during the manufacture, and are determined either by the magnitude of the elastic deformations that appear when cutting parts, or by X-ray analysis. The occurrence of type II residual stresses is attributed to the inhomogeneity of plastic deformations at the level of polycrystal grains. These stresses are balanced on the scale of one crystallite (grain). Residual stresses of type III are typical for the level of substructures (barriers, microdamages, complex dislocation structures) and are balanced on the scales of several crystalline cells [42, 39].

In this paper, we introduce the concept of residual mesostresses (RMS) that are self-balanced at the level of a representative macrovolume; these stresses are not included in the generally accepted classification. In modeling RMS, a representative volume should be unloaded after the stage of active elastoviscoplastic loading. Moreover, it should be borne in mind that the two-level model applied here is based on the Voigt hypothesis, and therefore it is intended for specifying loading conditions kinematically. For this reason, we need an iterative procedure that, under kinematic loading applied in strain increments, will ensure the fulfillment of $\mathbf{K}=\mathbf{0}$ to the required accuracy at the end of the unloading stage. That means that the weighted Kirchhoff stress tensor averaged over a representative volume must be equal to zero.

Let us now describe the unloading procedure for a representative macrovolume. We suppose that at an arbitrary (preceding) loading stage the macrostresses $\mathbf{K}$ occur in a representative macrovolume.

Then, to implement a step-by-step procedure, we write the transposed velocity gradient as

$$\hat{\nabla}\mathbf{V}^{\mathrm{T}}=-\chi\frac{\mathbf{K}}{\|\mathbf{K}\|},\quad \|\mathbf{K}\|=\left(\mathbf{K}:\mathbf{K}\right)^{1/2}, \tag{6}$$

where χ (s^{-1}) is the parameter related to the time step size to be determined numerically.

At the same time, due to the well-known problem of ambiguous definition of the unloaded configuration that can be established only up to rotation of the studied volume as a rigid whole, it is assumed that the main axes of the tensor $\mathbf{K}$ (or the elastic macrostrain tensor) remain unchanged during unloading. It should be noted that, although the unloading of the entire volume of a representative macrovolume is elastic, its separate crystallites can experience irreversible deformations. That is the reason why we have to use a step-by-step procedure in this study. The unloading process is considered completed if the $\|\mathbf{K}\|<\varepsilon$ (ε - small positive number) condition is fulfilled.

5. The results of numerical experiments

The purpose of the numerical experiments conducted here is to analyze the differences in macro- and meso-parameters when anisotropic properties are replaced by equivalent isotropic properties gained in simple shear, complex loading and cyclic deformation tests on materials with bcc, fcc, hcp lattices and different crystallite orientation distributions.

Two series of experiments were conducted. In the first experiments, the distribution of crystallite orientations in each sample is assumed to obey the uniform law. The sample consists of many crystallites with anisotropic or equivalent isotropic properties for each type of lattice. All samples are studied in three loading modes described by relations (3)–(5). The second series differs from the first one by the non-uniform orientation distribution functions corresponding to rolling textures. For the materials with hcp lattices, the distribution function was taken from [36] and, for materials with bcc and fcc lattices from [37].

During the first experiments (uniform crystallite orientation law in the reference configuration), we determined the macro- and meso SSS parameters in the framework of the model representing the material with anisotropic elastic properties for bcc, fcc and hcp lattices and for the samples with same crystal lattice arrangement, size and orientation and having equivalent isotropic elastic properties [28-30].

The samples from each of the groups (samples with anisotropic properties of crystallites and three macrosamples with isotropic properties of crystallites) were loaded according to the programs described by relations (3)–(5). After the intensity of the accumulated deformation reached 50%, the test sample was unloaded to zero values of the macrolevel stress intensity. The initial data and loading programs in the second series of experiments were similar to those of the first series, except for the non-uniform orientation distributions specified by the corresponding laws.

Under simple shear, the SSS curves for the sample with anisotropic elastic properties turned out to be close to the results obtained for the sample with effective isotropic properties, which were assumed to coincide with the averaged elastic characteristics of the polycrystalline sample with the uniform crystallite orientation distribution for both bcc and fcc lattices. At the same time, there is a segment with curve deviations, namely, a part corresponding to the transition of the sample from elastic to elastoplastic state. The analysis of the results of the computational experiment on complex monotonic loading implemented according to the law (4) indicates that the calculated stress-strain curves practically coincide for all types of lattices (Fig. 4). Only slight deviations happen in the elastoplasticity region after a sharp change in the type of loading, carried out when a certain value of the accumulated strain intensity reaches 5%. The smallest difference between the results (from the data for the sample with anisotropic properties) at the mesolevel was observed for the sample made of an equivalent isotropic material the elastic characteristics of which were obtained by the Voigt averaging.

Under cyclic loading specified by relation (5), the polycrystalline sample with uniform crystallite orientation distribution demonstrates the most significant deviations of the SSS curves for the hcp lattice (Fig. 5). The samples with bcc and fcc lattices are characterized by an almost complete coincidence of the dependences of stress intensity on the accumulated strain intensity. It is interesting that, despite the periodicity of the prescribed change in the deformed state, the stress intensity dependence does not exhibit such behavior, which is a consequence of the changes accumulated by the mesostructural parameters (changes in the orientation of crystallite lattices, shears and hardening on slip systems) that affect the response.

Strength characteristics, along with residual stresses, significantly depend on the type of stress state. In most works, a loading stiffness parameter (triaxiality factor) is used to characterize the type of stress state. This parameter is equal to the ratio of average stress to stress intensity:

$$\Theta = \frac{\kappa_{cp}}{\kappa_u}, \quad \kappa_{cp} = \frac{\mathrm{I}_1(\boldsymbol{\kappa})}{3}, \quad \kappa_u = \left(\frac{3}{2}\boldsymbol{\kappa}' : \boldsymbol{\kappa}'\right)^{1/2}, \tag{7}$$

where $\mathrm{I}_1(\cdot)$ is the first invariant of the second rank tensor, and $\boldsymbol{\kappa}'$ is the Kirchhoff stress deviator $\boldsymbol{\kappa}$.

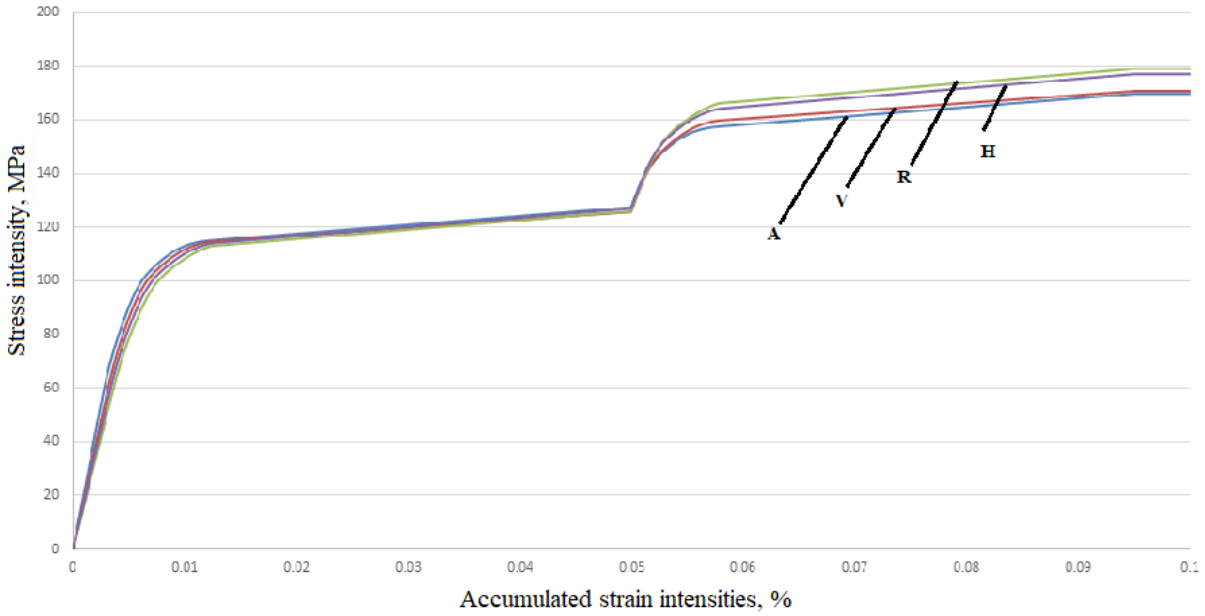

Fig.4. Dependences of stress intensities on accumulated strain intensities in polycrystal samples with fcc lattices under complex loading and at uniform crystallite orientation distribution obtained for materials with various properties by different averaging techniques: anisotropic material at the mesolevel (curve A); isotropic, Voigt average (V); isotropic, Reuss average (R); isotropic, Hill average (H).

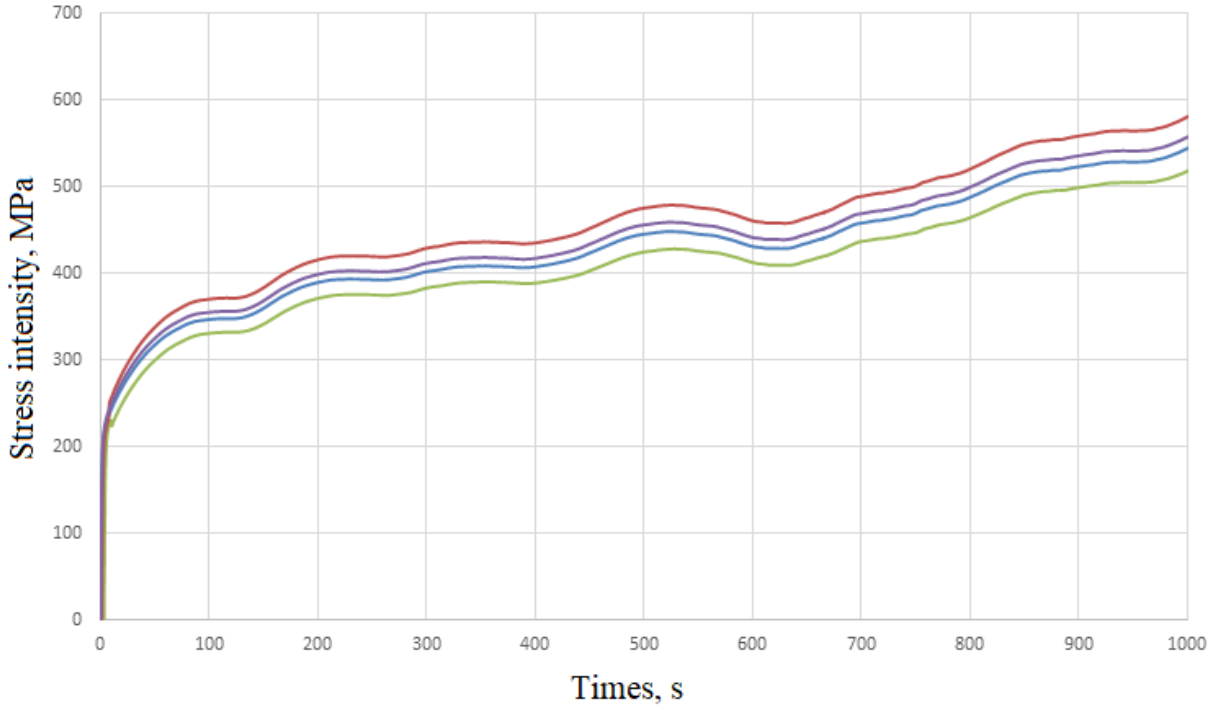

Fig.5 Time dependences of stress intensities of materials with hcp lattice under cyclic deformation and uniform crystallite orientation distribution (the notation is the same as in Fig.4).

Normal stresses can be tensile or compressive, and therefore materials fail differently. As experiments show, all materials, without exception, are capable of absorbing very high stresses under all-round compression, while, under all-round tension, the failure occurs at relatively low stresses. More information about the failure criteria can be found in numerous monographs (see, for example, [43–45]) and in the review paper [46].

Let us recall that this paper is focused on the model describing (with varying degrees of accuracy) the inherent properties in real objects. The purpose of the study is to compare the parameters of the samples made of the material with anisotropic elastic properties at the mesolevel and those of the

samples in which the elastic properties at the mesolevel are isotropic and determined by one of the averaging techniques (Voigt (V), Reuss (R), or Hill (H)). For all representative macrovolume crystallites, we determined the differences between the components of the residual stress tensors of anisotropic and corresponding isotropic crystallites $\left(\Delta\boldsymbol{\kappa}_{N\,m}\right)_{ij}$, where $N=\mathrm{V},\mathrm{R},\mathrm{H}$, the values of triaxility parameters, and the intensities of stress differences $\Delta\kappa_{N\,m}$, where $m=\overline{1,M}$, and M is the number of representative macrovolume mesolevel elements. To compare the results, we used the intensities of the differences between the residual mesostress tensors $\Delta\kappa_{N\,m}=\left(\frac{3}{2}\left(\boldsymbol{\kappa}'^{\mathrm{A}}_m-\boldsymbol{\kappa}'^{N}_m\right):\left(\boldsymbol{\kappa}'^{\mathrm{A}}_m-\boldsymbol{\kappa}'^{N}_m\right)\right)^{1/2}$, where $\boldsymbol{\kappa}'^{\mathrm{A}}_m$, $\boldsymbol{\kappa}'^{N}_m$ are the residual stress deviators in the m-th crystallite calculated for anisotropic (A) and isotropic elastic materials with corresponding average $N=\mathrm{V},\mathrm{R},\mathrm{H}$.

We have identified these pairs of crystallites in the materials the elastic properties of which are different but all other parameters are identical. In other words, the same crystallite exists in the original virtual material, which differs from the other two only by elastic - isotropic or anisotropic – properties. Under these circumstances, the intensity of the differences between the Kirchhoff stress deviators in the sample is maximum in the norm: $\left\|\Delta\kappa_N\right\|=\max\limits_{m=1,M}\Delta\kappa_{N\,m}$.

Table 2 includes the results of the calculations for the case when the polycrystalline samples with uniform crystallite orientation distribution are subjected to cyclic loading; the pairs of crystallites are identified according to the norm introduced above. The results indicate significant differences in the intensities of residual mesostresses and their components; the residual mesostress difference can even exceed the yield strength (in the reference configuration).

Table 2. Characteristics of residual mesostresses in the polycrystal samples made of anisotropic and isotropic elastic materials at a uniform law of orientation distribution of crystallites in the reference configuration under cyclic deformation.

	Compared materials								
	A and V			A and R			A and H		
Lattice	$\left\|\Delta\kappa_{\mathrm{V}}\right\|$, MPa	$\frac{\Theta_{\mathrm{V}}}{\Theta_{\mathrm{A}}}$	$\left(\Delta\boldsymbol{\kappa}_{\mathrm{V}}\right)_{ij}$, MPa	$\left\|\Delta\kappa_{\mathrm{R}}\right\|$, MPa	$\frac{\Theta_{\mathrm{R}}}{\Theta_{\mathrm{A}}}$	$\left(\Delta\boldsymbol{\kappa}_{\mathrm{R}}\right)_{ij}$, MPa	$\left\|\Delta\kappa_{\mathrm{H}}\right\|$, MPa	$\frac{\Theta_{\mathrm{H}}}{\Theta_{\mathrm{A}}}$	$\left(\Delta\boldsymbol{\kappa}_{\mathrm{H}}\right)_{ij}$, MPa
BBC	89,14	$\frac{0,61}{0,52}$	$\begin{pmatrix}24,74 & 17,42 & -19,57\\ 17,42 & 39,08 & 25,93\\ -19,57 & 25,93 & 21,01\end{pmatrix}$	98,57	$\frac{0,58}{0,52}$	$\begin{pmatrix}12,39 & 16,25 & -21,62\\ 16,25 & 46,54 & 24,5\\ -21,62 & 24,5 & 38,67\end{pmatrix}$	104,98	$\frac{0,46}{0,52}$	$\begin{pmatrix}28,13 & 19,9 & -34,4\\ 19,9 & 37,17 & 18,4\\ -34,1 & 18,4 & -36,87\end{pmatrix}$
FFC	67,42	$\frac{0,72}{0,64}$	$\begin{pmatrix}14,18 & 12,94 & -26,1\\ 12,94 & 24,08 & 13,7\\ -26,1 & 13,7 & 13,3\end{pmatrix}$	78,57	$\frac{0,58}{0,64}$	$\begin{pmatrix}24,91 & 13,4 & -15,6\\ 13,4 & 38,21 & 16,14\\ -15,6 & 16,14 & 25,85\end{pmatrix}$	74,93	$\frac{0,70}{0,64}$	$\begin{pmatrix}6,28 & 14,9 & -18,1\\ 14,9 & 23,57 & 21,08\\ -18,1 & 21,08 & 34,07\end{pmatrix}$
HCP	114,18	$\frac{0,68}{0,55}$	$\begin{pmatrix}15,47 & -31,27 & 16,62\\ -31,27 & 44,23 & 15,12\\ 16,62 & 15,12 & -59,42\end{pmatrix}$	120,23	$\frac{0,49}{0,55}$	$\begin{pmatrix}4,99 & -50,63 & -35,13\\ -50,63 & 24,79 & 16,32\\ -35,13 & 16,32 & -29,5\end{pmatrix}$	166,88	$\frac{0,61}{0,55}$	$\begin{pmatrix}9,31 & -40,62 & -3,18\\ -40,62 & 81,69 & 11,3\\ -3,18 & 11,3 & -90,73\end{pmatrix}$

We have analyzed the behavior of samples subjected to loads specified by laws (3)–(5) and the above inhomogeneous distributions of initial orientations corresponding to rolling textures. This led us to conclude that, for the polycrystalline samples with fcc lattice, the stress intensity–accumulated strain intensity curves (4) deviate only slightly, and, for the hcp polycrystals, the differences somewhat exceed the deviations shown in Figure 4. For the “stress intensity–accumulated strain intensity” curves obtained for the materials loaded according to the law (5), there are no visible discrepancies from the results presented in Figure 5. Therefore, of greater interest are the calculated data for mesolevel residual stresses, which are summerized in Table 3.

Table 3. Characteristics of residual mesostresses in the polycrystal samples made of anisotropic and isotropic elastic materials with uniform orientation distribution in the reference configuration under cyclic deformation.

Compared materials									
	A and V			A and R			A and H		
Lattice	$\|\Delta\kappa_V\|$, MPa	$\frac{\Theta_V}{\Theta_A}$	$(\Delta\boldsymbol{\kappa}_V)_{ij}$, MPa	$\|\Delta\kappa_R\|$, MPa	$\frac{\Theta_R}{\Theta_A}$	$(\Delta\boldsymbol{\kappa}_R)_{ij}$, MPa	$\|\Delta\kappa_H\|$, MPa	$\frac{\Theta_H}{\Theta_A}$	$(\Delta\boldsymbol{\kappa}_H)_{ij}$, MPa
BBC	94,63	$\frac{0,73}{0,66}$	$\begin{pmatrix} 37,28 & 19,93 & -21,42 \\ 19,93 & 51,37 & 18,27 \\ -21,42 & 18,27 & 33,67 \end{pmatrix}$	78,54	$\frac{0,81}{0,66}$	$\begin{pmatrix} 27,45 & 11,19 & -31,15 \\ 11,19 & 32,40 & 17,79 \\ -31,15 & 17,79 & 32,88 \end{pmatrix}$	124,71	$\frac{0,84}{0,66}$	$\begin{pmatrix} 36,94 & 14,07 & -26,86 \\ 14,07 & 29,42 & 24,63 \\ -26,86 & 24,63 & 29,09 \end{pmatrix}$
FFC	71,12	$\frac{0,67}{0,57}$	$\begin{pmatrix} 23,91 & 18,58 & -29,42 \\ 18,58 & 37,96 & 21,37 \\ -29,42 & 21,37 & 26,28 \end{pmatrix}$	82,08	$\frac{0,69}{0,57}$	$\begin{pmatrix} 17,97 & 24,18 & -29,08 \\ 24,18 & 34,68 & 27,62 \\ -29,08 & 27,62 & 37,13 \end{pmatrix}$	94,47	$\frac{0,63}{0,57}$	$\begin{pmatrix} 19,51 & 31,47 & -10,59 \\ 31,47 & 37,60 & 19,74 \\ -10,59 & 19,74 & 41,03 \end{pmatrix}$
HCP	127,97	$\frac{0,74}{0,61}$	$\begin{pmatrix} 39,11 & -17,97 & 17,02 \\ -17,97 & 43,15 & 26,12 \\ 17,02 & 26,12 & -18,31 \end{pmatrix}$	115,14	$\frac{0,76}{0,61}$	$\begin{pmatrix} 46,74 & 37,51 & -39,28 \\ 37,51 & 32,92 & 27,83 \\ -39,28 & 27,89 & 43,63 \end{pmatrix}$	144,58	$\frac{0,81}{0,61}$	$\begin{pmatrix} 37,91 & 42,07 & -14,82 \\ 42,07 & 56,29 & 23,35 \\ -14,82 & 23,35 & -61,21 \end{pmatrix}$

6. Conclusion

A two-level elastoviscoplastic model for studying processes of deformation of polycrystalline samples is described, as well as an algorithm for its implementation, and the results of computational experiments performed in the framework of this model, are presented. The samples considered in the study were made of isotropic and anisotropic elastic materials with different types of crystal lattice and investigated at various laws of crystallite orientation distributions and under different loading programs.

The results of the simulations demonstrate that, for the elastic materials made of polycrystals with uniform orientation distribution, the best agreement between the numerical data on macrolevel SSS, calculated for isotropic and anisotropic material characteristics, is achieved in polycrystalline samples with bcc and hcp lattices under simple shear. Under complex loading, the largest discrepancy occurs between the results determined for the polycrystalline samples from materials with an fcc lattice and those for the corresponding elastically isotropic samples produced from the materials with the elastic characteristics specified by the Reuss and Hill method, and the smallest deviations occur when using the Voigt averaging.

In modeling cyclic loading, the best approximation corresponds to the Hill averaging of the elastic characteristics of hcp polycrystals. However, the differences in residual mesostresses can reach great values (50–70% of the yield strength), which have a significant effect on the mesolevel stress state and the strength properties of products during operation. For the samples of polycrystalline materials with initial textures under approproate loading regimes, results similar to those described above were obtained.

The study was financially supported by the Russian Science Foundation (grant no. 17-19-01292).

References

1. Kachanov L.M. *Osnovy teorii plastichnosti* [Bases of the theory of plasticity]. Moscow, Nauka, 1969. 420 p.
2. Malinin N.N. *Prikladnaya teoriya plastichnosti i polzuchesti* [Applied theory of plasticity and creep]. Moscow, Mashinostroyeniye, 1975. 400 p.
3. Unksov E.P., Ovchinnikov A.G. (eds.) *Teoriya plasticheskikh deformatsiy metallov* [Theory of plastic deformations of metals] Moscow, Mashinostroyeniye, 1983. 598 p.
4. Vasin R.A. Opredelyayushchiye sootnosheniya teorii plastichnosti [Defining relations of the theory of plasticity]. *Itogi nauki i tekhniki. Ser. Mekhanika tverdykh deformiruyemykh tel*, 1990, vol. 21, pp. 3-75.
5. Il'yushin A.A. *Plastichnost'. Ch. 1. Uprugo-plasticheskiye deformatsii* [Plasticity. Part 1. Elastic-plastic deformations]. Moscow, Logos, 2004. 388 p.

6. Il'yushin A.A. *Trudy (1946–1966). T. 2. Plastichnost'* [Proceedings (1946–1966). Vol. 2. Plasticity]. Moscow, Fizmatlit, 2004. 480 p.
7. Horstemeyer M.F. Multiscale modeling: A review // Practical aspects of computational chemistry, ed. J. Leszczynski, M.K. Shukla. Springer, 2009. Pp. 87-135. https://doi.org/10.1007/978-90-481-2687-3_4
8. McDowell D.L. A perspective on trends in multiscale plasticity. *Int. J. Plast.*, 2010, vol. 26, pp. 1280-1309. https://doi.org/10.1016/j.ijplas.2010.02.008
9. Roters F. *Advanced material models for the crystal plasticity finite element method: Development of a general CPFEM framework.* Aachen, RWTH Aachen, 2011. 226 p.
10. Trusov P.V., Shveykin A.I., Nechaeva E.S., Volegov P.S. Multilevel models of inelastic deformation of materials and their application for description of internal structure evolution. *Phys. mesomech.*, 2012, vol. 15, pp. 155-175. https://doi.org/10.1134/S1029959912020038
11. Trusov P.V., Shveykin A.I. *Mnogourovnevyye modeli mono- i polikristallicheskikh materialov: teoriya, algoritmy, primery primeneniya* [Multilevel models of mono- and polycrystalline materials: theory, algorithms, application examples]. Novosibirsk, Silberian Branch of RAS, 2019. 605 p
12. Taylor G.I. Plastic strain in metals. *J. Inst. Metals*, 1938, vol. 62, pp. 307-324.
13. *Lin T.H.* Analysis of elastic and plastic strains of a face-centered cubic crystal // J. Mech. Phys. Solid. 1957. Vol. 5. P. 143-149. https://doi.org/10.1016/0022-5096(57)90058-3
14. Sokolov A.S., Trusov P.V. Two-level elastic-viscoplastic model: application to the analysis of the crystal anisotropy influence. *Vychisl. mekh. splosh. sred – Computational continuum mechanics*, 2020, vol. 13, no. 2, pp. 219-230. https://doi.org/10.7242/1999-6691/2020.13.2.17
15. Pozdeyev A.A., Trusov P.V., Nyashin Yu.I. *Bol'shiye uprugoplasticheskiye deformatsii: teoriya, algoritmy, prilozheniya* [Large elastic-plastic strains: theory, algorithms, applications]. Moscow, Nauka, 1986. 232 p.
16. Trusov P.V., Shveykin A.I., Yanz A.Yu. Motion decomposition, frame-indifferent derivatives, and constitutive relations at large displacement gradients from the viewpoint of multilevel modeling. *Phys. Mesomech.*, 2017, vol. 20, pp. 357-376. https://doi.org/10.1134/S1029959917040014
17. Trusov P.V., Shveykin A.I. On motion decomposition and constitutive relations in geometrically nonlinear elastoviscoplasticity of crystallites. *Phys. Mesomech.*, 2016, vol. 19, pp. 377-391. https://doi.org/10.1134/S1029959917040026
18. Lurie A.I. *Nonlinear theory of elasticity*. Elsevier, 1990. 617 p.
19. Kroner E. Allgemeine Kontinuumstheorie der Versetzungen und Eigenspannungen [Continuum theory of dislocations and residual stresses]. *Arch. Rational Mech. Anal.*, 1959, vol. 4, pp. 273-334. https://doi.org/10.1007/BF00281393
20. Lee E.H. Elastic-plastic deformation at finite strain. *J. Appl. Mech.*, 1969, vol. 36, pp. 1-6. https://doi.org/10.1115/1.3564580
21. Zhang Z., Cuddihy M.A., Dunne F.P.E. On rate-dependent polycrystal deformation: the temperature sensitivity of cold dwell fatigue. *Proc. R. Soc. A*, 2015, vol. 471, 20150214. https://doi.org/10.1098/rspa.2015.0214
22. Feng B., Bronkhorst C.A., Addessio F.L., Morrow B.M., Cerreta E.K., Lookman T., Lebensohn R.A., Low T. Coupled elasticity, plastic slip, and twinning in single crystal titanium loaded by split-Hopkinson pressure bar. *J. Mech. Phys. Solid.*, 2018, vol. 119, pp. 274-297. https://doi.org/10.1016/j.jmps.2018.06.018
23. Zhang Z., Jun T.-S., Britton T.B., Dunne F.P.E. Determination of Ti-6242 α and β slip properties using micro-pillar test and computational crystal plasticity. *J. Mech. Phys. Solid.*, 2016, vol. 95, pp. 393-410. https://doi.org/10.1016/j.jmps.2016.06.007
24. Zhang Z., Jun T.-S., Britton T.B., Dunne F.P.E. Intrinsic anisotropy of strain rate sensitivity in single crystal alpha titanium. *Acta Mater.*, 2016, vol. 118, pp. 317-330. https://doi.org/10.1016/j.actamat.2016.07.044
25. Matsyuk K.V., Trusov P.V. Model for description of viscoelastoplastic deformation of hcp crystals: asymmetric stress measures, hardening laws. *Vestnik PNIPU. Mekhanika – PNRPU Mechanics Bulletin*, 2013, no. 4, pp. 75-105. https://doi.org/10.15593/perm.mech/2013.4.75-105
26. Wu X., Kalidindi S.R., Necker C., Salemet A.A. Modeling anisotropic stress-strain response and crystallographic texture evolution on α-titanium during large plastic deformation using Taylor-type models: Influence of initial texture and purity. *Metall. Mater. Trans. A*, 2008, vol. 39, pp. 3046-3054. https://doi.org/10.1007/S11661-008-9651-X
27. Kondratev N.S., Trusov P.V. A mathematical model for deformation of BCC single crystals taking into consideration the twinning mechanism. *Vychisl. mekh. splosh. sred – Computational continuum mechanics*, 2011, vol. 4, no. 4, pp. 20-33. https://doi.org/10.7242/1999-6691/2011.4.4.36
28. Shermergor T.D. *Teoriya uprugosti mikroneodnorodnykh tel* [The theory of elasticity of micro-inhomogeneous bodies]. Moscow, Nauka, 1977. 399 p.

29. Hirth J., Lothe J. *Theory of Dislocations*. McGraw-Hill, 1968. 780 p.
30. Newnham R.E. *Properties of materials. Anisotropy, symmetry, structure*. Oxford University Press, 2005. 390 p.
31. Man C.-S., Huang M. A simple explicit formula for the Voigt-Reuss-Hill average of elastic polycrystals with arbitrary crystal and texture symmetries. *J. Elast.*, 2011, vol. 105, pp. 29-48. https://doi.org/10.1007/s10659-011-9312-y
32. Krivosheina M.N., Tuch E.V., Khon Yu.A. Applying the Mises-Hill criterion to modeling the dynamic loading of highly anisotropic materials. *Bull. Russ. Acad. Sci. Phys.*, 2012, vol. 76, pp. 80-84. https://doi.org/10.3103/S1062873812010169
33. Krivosheina M.N., Kobenko S.V., Tuch E.V. Averaging of properties of anisotropic structural materials in numerical simulation of their fracture. *Phys. Mesomech.*, 2010, vol. 13, no. 2, pp. 55-60.
34. Raab G.I., Aleshin G.N., Fakhredinova E.I., Raab A.G., Asfandiyarov R.N., Aksenov D.A., Kodirov I.S. Prospects of development of new pilot-commercial SPD methods. *MTD*, 2019, vol. 1, no. 1, pp. 48-57.
35. Raab G.I., Kodirov I.S., Aleshin G.N., Raab A.G., Tsenev N.K. Influence of special features of the gradient structure formation during severe plastic deformation of alloys with different types of a crystalline lattice. *Vestnik MGTU im. G.I. Nosova – Vestnik of Nosov Magnitogorsk State Technical University*, 2019, vol. 17, no. 1, pp. 64-75. https://doi.org/10.18503/1995-2732-2019-17-1-64-75
36. Hama T., Kobuki A., Takuda H. Crystal-plasticity finite-element analysis of anisotropic deformation behavior in a commercially pure titanium Grade 1 sheet. *Int. J. Plast.*, 2017, vol. 91, pp. 77-108. https://doi.org/10.1016/j.ijplas.2016.12.005
37. Ji Y.T., Suo H.L., Ma L., Wang Z., Yu D., Shaheen K., Cui J., Liu J., Gao M.M. Formation of recrystallization cube texture in highly rolled Ni–9.3 at % W. *Phys. Metals Metallogr.*, 2020, vol. 121, pp. 248-253. https://doi.org/10.1134/S0031918X20020180
38. Birger I.A. *Ostatochnyye napryazheniya* [Residual stresses]. Moscow, Mashgiz, 1963. 232 p.
39. Pozdeyev A.A., Nyashin Yu.I., Trusov P.V. *Ostatochnyye napryazheniya: teoriya i prilozheniya* Residual stresses: theory and applications]. Moscow, Nauka, 1974. 112 p.
40. Birger I.A., Shor B.F., Iosilevich G.V. *Raschet na prochnost' detaley mashin* [Calculation of the strength of machine parts]. Moscow, Mashinostroyeniye, 1979. 702 p.
41. Abramov V.V. *Ostatochnyye napryazheniya i deformatsii v metallakh* [Residual stresses and deformations in metals]. Moscow, State Scientific and Technical Publishing House of Machine-building literature, 1963. 356 p.
42. Fridman Ya.B. *Mekhanicheskiye svoystva metallov. Ch. 1. Deformatsiya i razrusheniye* [Mechanical properties of metals. Part 1. Deformation and Destruction]. Moscow, Mashinostroyeniye, 1974. 472 p.
43. Kachanov L.M. *Osnovy mekhaniki razrusheniya* [Fundamentals of fracture mechanics]. Moscow, Nauka, 1974. 312p.
44. Collins J.A. *Failure of materials in mechanical design: Analysis, prediction, prevention*. John Wiley & Sons, 1981. 629 p.
45. Rabotnov Yu.N. *Vvedeniye v mekhaniku razrusheniya* [Introduction to fracture mechanics]. Moscow, Nauka, 1987. 80 p.
46. Besson J. Continuum models of ductile fracture: A Review. *Int. J. Damage Mechanics*, 2010, vol. 19, pp. 3-52. https://doi.org/10.1177/1056789509103482

The authors declare no conflict of interests.
The paper was received on 1.10.2021.
The paper was accepted for publication on 3.11.2021.